Number 60 | November 2022

SWISS NEUTRON NEWS

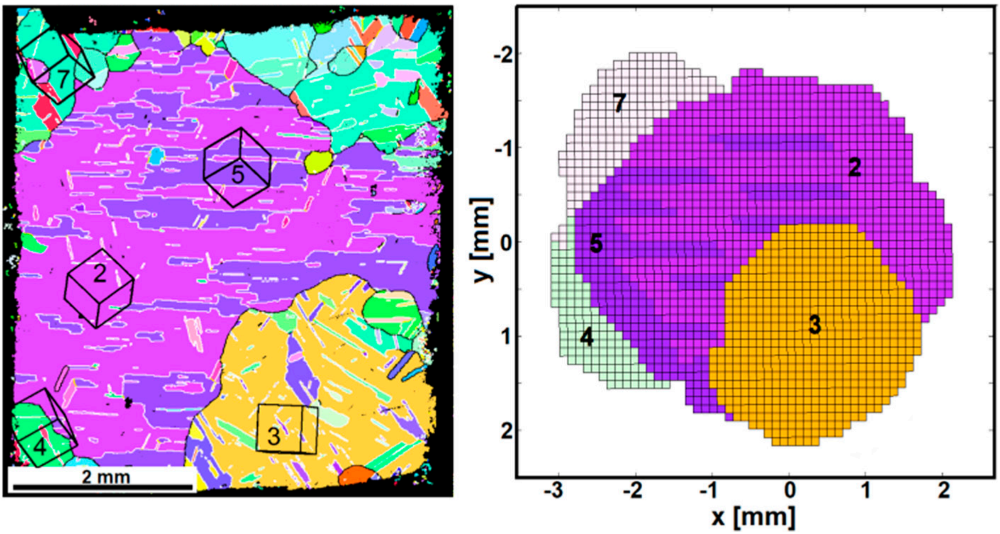

Schweizerische Gesellschaft für Neutronenforschung
Société Suisse de la Science Neutronique
Swiss Neutron Science Society

On the cover

EBSD map of a Cu sample taken at 3.2 mm from the surface of the sample (left) and the corresponding slice from Laue 3DNDT morphology reconstruction (right). The grains for both EBSD and Laue 3DNDT are numbered according to the Laue indexing order and are colour-coded in accordance with their orientation based on the inverse pole figure colour map for a top view on the specimen. The orientation of the unit cell in space is also give for every grain in the EBSD map.

by S. Samothrakitis, C. B. Larsen, M. Raventós, E. Polatidis, J. Čapek, S. Schmidt and M. Strobl

Contents

The President's Page

Dear fellow neutron scientists,

The year 2022 has been tremendously successful and rewarding for neutron science in Switzerland. Notably, several neutron scientists who either currently work at Swiss Institutions or have previously carried out key projects at Swiss institutions were recognized with awards for their outstanding contributions to neutron science on the international stage.

In August, at the International Conference on Neutron Scattering (ICNS) in Argentina, the European Neutron Scattering Association (ENSA) awarded Ellen Fogh, currently a postdoctoral researcher at EPFL, with the Erwin Felix Lewy Bertaut Prize. With the award, ENSA recognizes her innovative work using the highest available magnetic fields to elucidate the complex links between magnetoelectricity and field-dependent magnetic structures. Further, ENSA awarded the Swiss scientist Peter Böni with the Walter Hälg Prize for his ground-breaking career-long contributions to superconductivity and magnetism using neutron scattering. The award also recognizes Peter for his contributions to neutron instrumentation and optics. These contributions are also key for the continuous success of the Swiss spallation neutron source SINQ at PSI. Also this summer, Artur Glavic from PSI was awarded the inaugural instrumentation prize by the German "Committee Research with Neutrons (KFN)". Artur received the award during the "German Conference for Research with Synchrotron Radiation, Neutrons and Ion Beams at Large Facilities (SNI2022) in recognition of his work on the reflectometer ESTIA for the European Spallation Source. Obviously, this speaks to the overall high quality of neutron research in Switzerland! Please join me in congratulating all the award winners!

Naturally, to maintain these high standards, it is crucial that we continue to invest in our future. The SNSS does this every year by awarding the Young Scientist prize to a young scientist in recognition of a notable scientific achievement in the form of a PhD thesis. This year we recognize the PhD work of Stephan Allenspach for his thesis work on "Quantum Criticality and Dimensionality in Quasi-2D Spin-Dimer Systems". Please also join me in congratulating Stephan who received the award at this year's annual meeting of the Swiss Physical Society, as part of a large award ceremony where he delivered a beautiful talk on his work (see photo).

I want to draw your attention to the new report "Neutron Science in Europe" published by the League of Advanced European Neutron Sources (LENS) in collaboration with BrightnESS2, which address the challenges and opportunities for European neutron science to remain a key contributor in addressing societal challenges. In this issue of Neutron News, you will find an interesting development that will help us address such challenges. It reports on how to employ the Fast Acquisition Laue Camera for Neutrons (FALCON) instrument to carry out three-dimensional neutron diffraction tomography.

I wish all of you the best for the remainder of the year and hope to see you at our general assembly.

Marc Janoschek

Laue three dimensional neutron diffraction tomography and the FALCON instrument

S. Samothrakitis[1], C. B. Larsen[1], M. Raventós[1], E. Polatidis[1], J. Čapek[1], S. Schmidt[2], M. Strobl[1]

Abstract

This article presents a measurement technique and data analysis tool to perform Laue 3-dimensional neutron diffraction tomography (Laue 3DNDT). The approach builds on utilizing the FALCON instrument and a forward model used for correlating and multiple fitting of the measured diffraction spots relative to individual grains. This enables not only to identify individual grains, but also their position and orientation in the sample. The article describes several science cases, with increasing analysis complexity, i.e. from oligocrystalline materials, to indexing the crystallographic orientation of several hundred grains in polycrystalline materials, which, thus, enables grain-resolved characterization of texture in the volume of centimeter-sized coarse-grained samples with statistical significance. The FALCON instrument is currently at PSI and further analysis efforts, with the use of advanced data science methods, are taken to optimize the analysis routines to increase the results yield and efficiency. The short exposure times and non-destructive nature of the Laue

three-dimensional neutron diffraction render it a novel promising method for corresponding characterization of a wide range of materials.

1. Introduction

The ability to determine non-destructively and in three-dimensions the microstructural characteristics of engineering and functional materials such as grain size, grain morphology and crystallographic texture, is essential to understanding the damage, deformation mechanisms and thermomechanical processes in polycrystalline metallic materials used in many technological applications. Classical methods for characterizing the microstructure usually involve viewing an image from a sectioned surface, where the area of interest is polished and viewed in an optical or scanning electron microscope (SEM). However, microstructural features such as grain size, morphology, phase interactions and interface boundaries cannot be inferred from 2D sections accurately. To this end, obtaining full 3D information of the microstructure makes it possible to characterize these properties more reliably. Furthermore, the spatially resolved information in each grain of the polycrystalline aggregate can be utilized to validate results of predictive models of crystal plasticity.

Accordingly, a wide range of characterization techniques, electron-based [1–6] and X-ray-based [7–14], exist and are being progressed continuously in order to provide access to full characterization of crystallographic structures, either from the surface or the bulk of samples. Methods, such as 3D electron backscattering diffraction and 3D X-ray diffraction, are increasingly used in grain orientation mapping with exciting prospects. However, the limited penetration of electrons and X-rays into relevant specimens, especially for elements with high atomic numbers, restricts representative studies of the bulk of many engineering and structural alloys.

The development of neutron-based three-dimensional characterization techniques [15–21] bears the potential for bulk studies of centimeter-sized samples. This is possible due to the superior penetration ability of neutrons into metallic specimens, offering the possibility to non-destructively probe large volumes and structures, deep in the bulk of engineering and functional materials.

A consortium between the Applied Material Group (AMG) at Paul Scherrer Institute (PSI) in Switzerland, the Technical University of Denmark - DTU and the Nuclear Physics Institute in the Czech Republic has developed and used the so-called Laue three-dimensional neutron diffraction tomography (Laue 3DNDT) method together with dedicated analysis algorithms. Some of the highlights utilizing this method are presented in Section 3. The detectors of the FALCON instrument, which was built and operated at the E11 beam port of the BER II reactor of Helmholtz-Zentrum Berlin (HZB), were transferred to the Paul Scherrer Institute in 2020 after the closure of BER II. In December 2021, the FALCON detectors were commissioned for use at the POLDI instrument, SINQ. In future, a full-scale instrument suitable also for routine Laue neutron diffraction at a dedicated position in the SINQ neutron guide hall will be built. With the establishment of FALCON at PSI, the Laboratory for Neutron Scattering and Imaging (LNS) expands its suite of instruments for condensed matter physics and materials science studies.

2. The Laue 3DNDT method, experiments and analysis

The experiments were performed using the Fast Acquisition Laue Camera for Neutrons (FALCON) instrument [22]. The FALCON system consists of two detectors; one for forward diffraction and one for back-diffraction. Each detector is composed of a ^{6}LiF-ZnS scintillator plate with a total surface area of 400 × 400 mm^2 and a thickness of 250 µm coupled with four iCCD cameras of 4000 × 4000 total pixel area (100 µm pixel size). A schematic of the setup is shown in Fig. 1a. Typically, Laue 3DNDT experiments are undertaken in a tomographic mode: as the sample is rotated, some sets of planes satisfy the Bragg condition for certain projections and new spots appear while others disappear in the Laue diffraction pattern for consecutive rotation steps; an example of the trajectories of the spots depending on the rotation angle is shown in Fig. 1b. The ω rotation (i.e. tomography) and the use of a white neutron beam make it possible to collect diffraction data from many *hkl* planes per crystallite, which in turn facilitates the analysis. The obtained

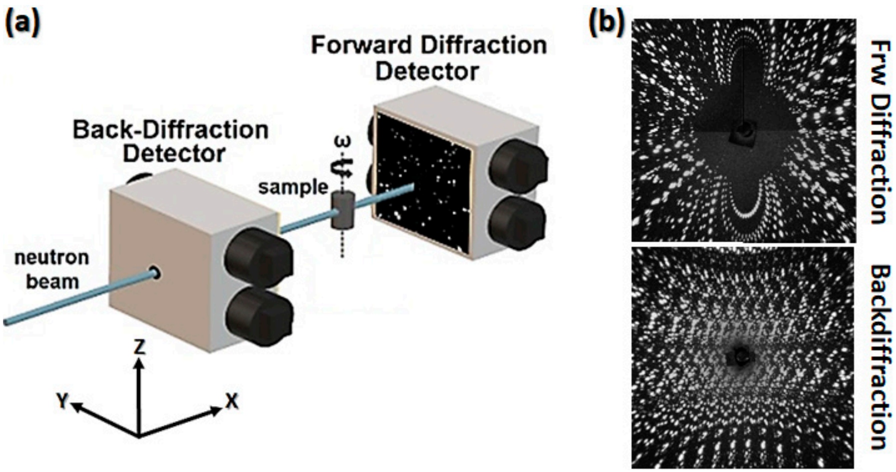

Fig. 1
(a) Schematic of the double detector Laue setup of the FALCON instrument. The neutron beam traverses the center of the backscattering detector through a 2 cm wide hole, illuminates the sample and diffracts, with the transmitted beam meeting the beam stop in front of the forward scattering detector. The schematic is adapted by [23]. (b) Example of the trajectories of the Bragg reflections, both in forward and back-diffraction, summed over an angular range of 360° and an angular step of 4°.

data for each measurement consist of several tens to hundreds of diffraction patterns containing numerous diffraction spots.

For the Laue 3DNDT measurements, a continuous white neutron beam (wavelength range of 0.8 Å - 3.2 Å at the E11 beamport, HZB and 0.9 - 4.1 Å at POLDI, PSI) oriented along the (horizontal) x-axis (see Fig. 1a) passes through the backscatter detector, illuminates the sample and produces Laue diffraction patterns on the backscattering and the forward scattering detectors. The two detectors are mounted normal to the x-axis and are positioned symmetrically before and after the sample, respectively, however, the sample-to-detector distances can be varied based on the needs of individual measurements.

The mathematical and methodological frameworks of Laue 3DNDT, for grain indexing and morphology reconstruction, have been presented in detail in Ref. [20] and [21], respectively. We will thus give only a short overview, highlighting the method's main features.

Post experimentally and prior to indexing, the median image of a full tomography dataset is subtracted from each recorded Laue pattern. This helps to reduce to a high degree background artifacts, such as electronic noise and the so-called skyshine, the latter resulting from the spread of the direct beam at the center of the detector. Binarization and segmentation of the diffraction spots are then performed by a combination of e.g. the Otsu binarization method [24] and adaptive thresholding [25]. In order to decrease spot-overlap and to minimize the impact of electronic noise, the segmentation is carried out with strict thresholding parameters; the adaptive threshold sensitivity and neighborhood size are kept low, in addition to setting a minimum limit to spot area and intensity, effectively discarding smaller, weak diffraction spots (and electronic noise) and reducing the size of larger diffraction spots.

Laue 3DNDT makes use of a broad continuous thermal neutron wavelength (polychromatic) spectrum. Consequently, the recorded diffraction signal is not wavelength-resolved and Bragg's equation cannot be directly used to retrieve information. As such, the method was developed based on forward modelling [26]. Given specific experimental parameters (i.e., wavelength range, detector size and overall setup) and sample parameters (crystal structure, possible grain positions and orientations), a range of different diffraction patterns are simulated and a library containing the patterns is constructed. Subsequently, every pattern in the library is compared against the experimental diffraction data. A grain is considered indexed once matching conditions between simulations and experiment are found and the fitting criteria are met.

Following indexing, the three-dimensional reconstruction of the grains' morphology is performed utilizing the ASTRA toolbox for tomographic reconstruction [27,28] in combination with a three-dimensional vector version of the Simultaneous Iterative Reconstruction Technique (SIRT) algorithm [29]. A 3D version of SIRT enables the reconstruction of the volumes of the grains from the 3D vector-defined projection datasets. The algorithm works by first reconstructing a volume by back projection, then forward projecting the volume in the same directions as the back projection, and iteratively minimizing the least square difference between the orig-

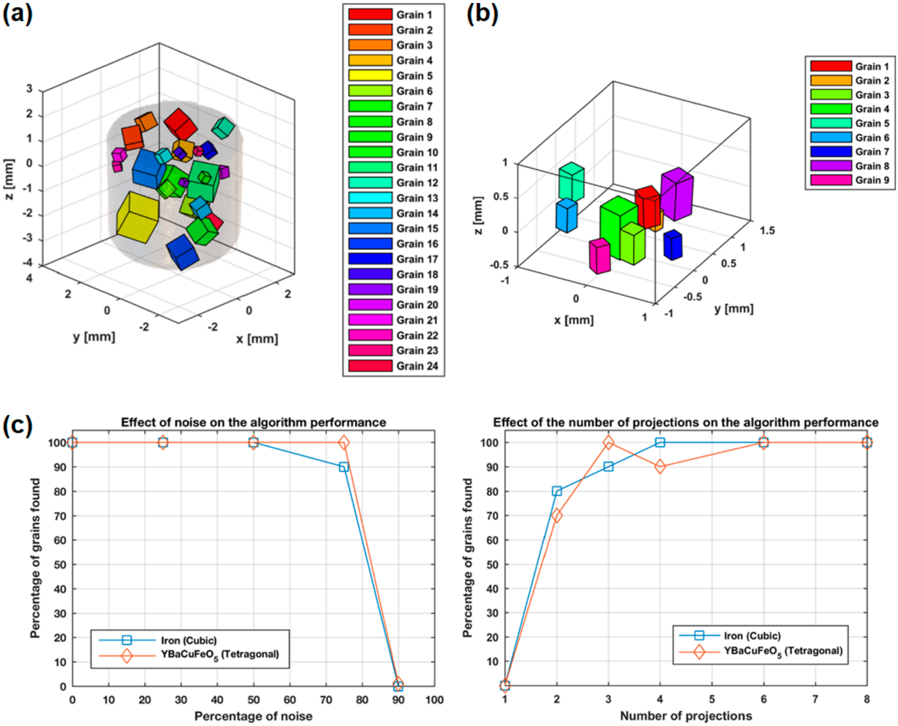

Fig. 2
(a) Iron sample of 5 mm diameter and 5 mm height, with low opacity overlaid with colored cubes representing the different grains and their and their orientations. (b) Plot with the 9 grains found by the algorithm inside the layered perovskite sample, represented by colored prisms representing the different grains and their orientations. The volume of the cubes in (a) and (b) is based on the integrated intensity of the diffraction spots of every grain and is proportional to the relative volume of the grain (c) Simulations results showing the number of grains found vs percentage of spots substituted (left) and the number of grains found vs number of angular steps for the measurement (right). Figure adapted by [20].

inal dataset and the forward-projection. The ASTRA toolbox provides high performance tools for Central Processing Unit (CPU) and Graphics Processing Unit (GPU) [30] for the latter task. The orientation and position of the indexed grains along with the shape and intensity of the corresponding reflections are used to create input parameters to the 3D grain morphology reconstruction process.

3. Results and examples

3.1 Grain orientation indexing - First results with Laue 3DNDT

The feasibility and performance of the Laue 3DNDT approach were tested by indexing multi-grain synthetic datasets from cubic (α-Fe) and tetragonal ($YBaCuFeO_5$) symmetries, providing benchmarks for robustness, precision and limitations of the method. Indexing of experimental datasets, collected from two different samples, was also performed. The first sample is a Fe oligocrystalline cylinder of 5 mm diameter and 5 mm height. The sample was measured using both forward and backward detectors with $\Delta\omega = 1°$ over 241° and 10 seconds of exposure time per angular step. The second sample is an oligocrystal of the high-temperature multiferroic candidate $YBaCuFeO_5$ with layered perovskite structure [31,32], in which several grains with a common *c*-axis and slightly different orientation in the ab plane were formed during the process of crystal growth [33]. The main objective concerning this sample was to identify the number of grains and the respective misalignment of the ‹001› direction, as well as the relative contribution of each domain to the diffracted signal (i.e., size distribution). The sample was measured using the forward detector with $\Delta\omega = 1°$ over 241° and 230 seconds of exposure time per angular step.

From the simulated data indexing we were able to retrieve the position and orientation of 97 out of 100 grains from the synthetic α-Fe data set. Further indexing of simulated data indicated that Laue 3DNDT is capable of indexing 10 out of 10 grains for both symmetries in two extreme scenarios: using only 6 Laue projections and using 360 projections with extremely noisy data. The precision achieved in terms of spatial and orientation resolution is 430 µm and 1°, respectively. Indexing of the experimental data returned 24 and 9 grains from the α-Fe and $YBaCuFeO_5$ samples, respectively. A summarised version of the results can be seen in Fig. 2.

3.2 Grain morphology reconstruction

For the grain morphology reconstruction two samples were measured in tomography mode; an Fe and a Cu oligocrystalline samples. The Fe sample is the same as the one used in the first indexing approach, presented by Raventos et al. [20] (see section 3.1).

Iterative forward modelling returned a total number of 24 grains, which were identified in the Fe sample. In the Cu sample 9 grains could be found and indexed. The reconstructed volumes of both samples, consisting of the reconstructed grains, are represented in Fig. 3, right hand side, alongside with a schematic representation of the grains, depicted as cubes around their found centre-of-mass positions (see Fig. 3, left hand side), for comparison. The relative volume of the cubes in the schematic depictions was calculated, as an estimate of the respective size of the grains, using the integrated intensities of the indexed peaks. It may be seen that this relative volume estimation is in good agreement with the results obtained by the morphological reconstruction, which takes into account only the shape of the indexed reflections. This may serve as an ad-hoc validation of the 3D reconstruction of the respective grain morphologies. The grain

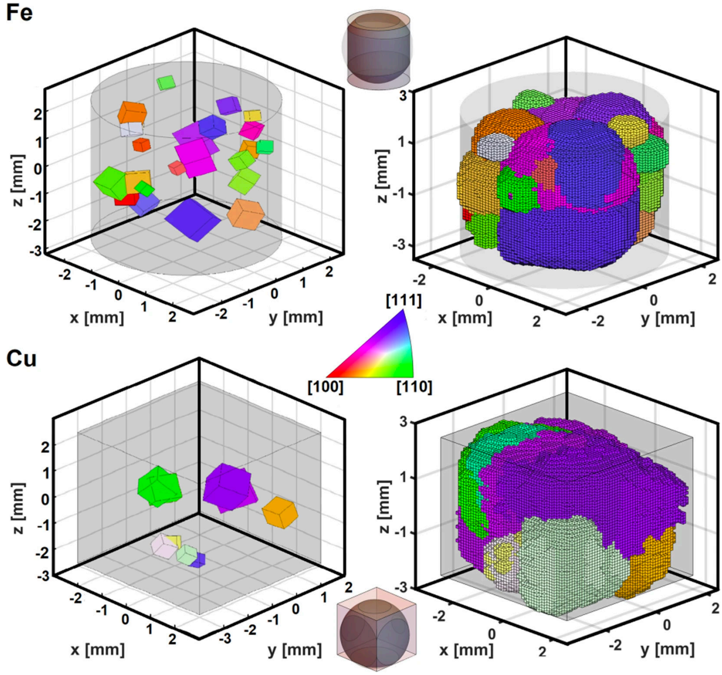

Fig. 3
Three-dimensional orientation (top and bottom left) and morphology (top and bottom right) maps of the crystal grains of the Fe and Cu samples, respectively. The grains are colour-coded in accordance with their orientation based on the inverse pole figure colour map for a top view (positive z-direction) on the specimen. The shaded areas around the grains represent the shape of each sample. The small schematics given at the top and bottom of the figure show the volume area of each sample that was effectively illuminated by the neutron beam [21].

morphology is fully reconstructed within the sample volume fully illuminated by the neutron beam. The respective probed volumes are depicted by insets in Fig. 3 through schematic illustrations of the respective gauge and sample volumes.

For actual validation of the approach, the Laue 3DNDT morphological reconstruction of the Cu sample was related to results obtained by post-mortem EBSD. Using the evaluated grain orientations and position from Laue 3DNDT, apart from the known sample geometry, it is possible to find a unique transformation that aligns the Laue 3DNDT reference system with that of the EBSD in order to identify the EBSD plane in the reconstructed sample volume. Two EBSD maps along with the identified corresponding slices from the Laue 3DNDT grain map are shown in Fig. 4. The grains reconstructed and identified in the two slices in Fig. 4 can clearly be associated and matched in shape, size and crystal-

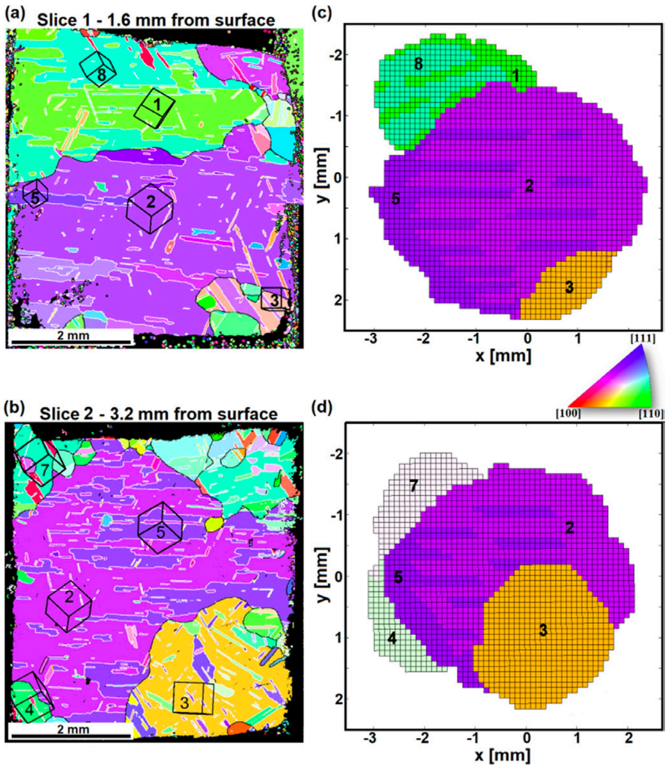

Fig. 4
Validation of the Laue 3DNDT grain morphology reconstruction. (a,b) EBSD maps of the Cu sample taken at 1.6 mm and 3.2 mm from the surface of the sample, respectively. (c,d) Corresponding slices from the Laue 3DNDT morphology reconstruction. The grains for both the EBSD and Laue 3DNDT are numbered according to the Laue indexing order and are colour-coded in accordance with their orientation based on the inverse pole figure colour map for a top view (positive z-direction) on the specimen. In (a,b) the grain orientation is also schematically depicted with the unit cells. The black lines surrounding the grains indicate grain boundaries, while white and yellow lines show twin and double twin boundaries, respectively. Colour variation within one image (for the same grain) is attributed to the shift of the electron beam due to the large area scanned. Small colour variations for the same grains from different EBSD scans originate from slight misalignment of the sample after removing and reinserting it into the SEM sample chamber [21].

lographic orientation, with those found in EBSD. An interesting aspect is the presence of twins indicated e.g. as grains 1 and 8 as well as 2 and 5. The EBSD map shows e.g. the existence of a big grain (grain 2 in light purple) in the central part that contains a number of twins, one of which (grain 5 in dark purple) is most pronounced. This parent-twin couple is identifiable as grains 2 and 5 in the Laue 3DNDT reconstruction, but the exact fine-structured interplay as in the EBSD cannot be resembled, due to resolution limits. However, from the neutron reconstruction it is found that the centres-of-mass of both of these two grains are in the centre of the sample having the highest calculated volume, which is well in agreement with the EBSD results.

3.3 High grain statistics for texture characterization

Laue 3DNDT was used for the characterization of a 1 cm^3 polycrystalline Fe-Ni-Mn austenitic alloy (nominal composition Fe-20.2Ni-5.4Mn wt. %) with face centered cubic (fcc) crystal structure, having estimated grain sizes in the order of a few hundred micrometres. During measurements, the sample was rotated and diffraction patterns were acquired for every angular step, Δω, for as large angular range, ω, as possible, in tomographic mode; an ω range from 0° to 320° was enabled and a total number of 33 projections with an increment of $\Delta\omega = 10°$ was recorded. An exposure time of 30 s per projection provided sufficient signal-to-noise ratio and resulted in a total measuring time of 16.5 min.

An unprecedented total number of 481 grains were successfully indexed in terms of crystallographic orientation, center-of-mass position, and relative size. The indexed grain aggregate of the sample, containing the 481 grains, is presented in Fig. 5, left hand side. The grains, depicted schematically as cubes, are positioned in space at their center-of-mass position. The size of the cubes is scaled according to their relative volume, estimated from the integrated intensities of the corresponding diffraction spots [34]. The cubes are colored based on their crystallographic orientations with respect to the positive z direction adopted from the inverse pole figure (IPF) coloring. The grain orientations are also indicated by the spatial inclination of the cubes. The grains occupy the illuminated volume area at the central part of the sample, which can be estimated to be about 50%–60% of the total sample volume. The characterized crystallographic orientation distribution is given in the form of IPFs along the z direction of the sample (see Fig. 5, right hand side). A uniform distribution of orientations is observed indicating random crystallographic texture.

Investigating the misorientation angles between neighboring indexed grains, allowed to reveal the presence of potential annealing twins in the microstructure. A total number of 9 twin-related grains were detected within the indexed sample volume. Among the indexed twins, 7 twin grains were found with a misorientation angle close to 60° with a ‹111› rotation axis, which is the basic twinning system for materials with fcc Bravais lattice. An extra 2 grains were found to have 2 twin variants, with the misorientation angle between parent and twin grains being close to 60° and that between the twin variants being 39° with a ‹110› rotation axis. Finally, the results were correlated with EBSD characterization and with a simulated randomly orientated microstructure [35]. Very good agreement was found in terms of distribution of misorientation axes, and the presence of twins was also verified.

The number of indexed grains is unparalleled by any earlier approach of neutron grain

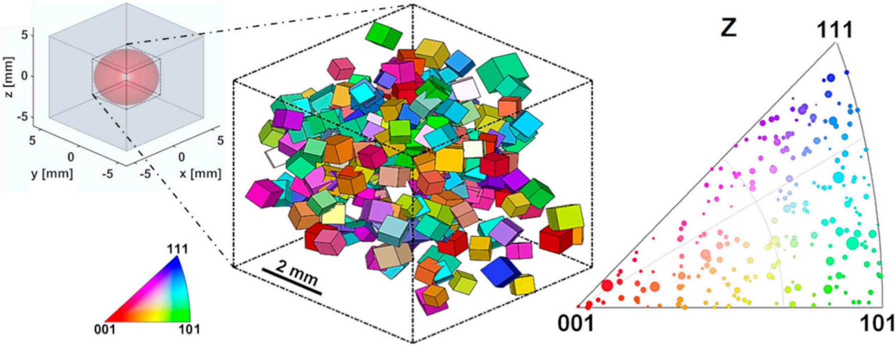

Fig. 5
Left - Laue 3DNDT map of the Fe-Ni-Mn grain volume, containing 481 indexed grains, depicted as cubes, in isoprojection. The grains are color-coded based on the inverse pole figure (IPF) color-map for a top view (positive z-direction) on the specimen. The cubes are also inclined, representing the orientation of the cubic unit cell within each grain in accordance to the crystallographic orientation. The size of the cubes is scaled based on their relative volume, as calculated from the intensities of the corresponding diffraction spots. The gray shaded volume in the top left schematic represents the sample with a volume of 1 × 1 × 1 cm^3 and the red sphere represents the beam profile and the gauge volume. Right - Inverse pole figures (IPF) along the Z direction showing the orientation distribution of the indexed grains [34].

mapping and allows revealing a nearly random crystallographic texture as shown in Fig. 5. A particular strength of the method are the shorter acquisition times, and a small number of required projections, especially when compared to prior neutron-based methods [17,19]. This method enables superior grain statistics than traditional EBSD, by probing a larger volume of grains. The ability to resolve a larger number of grains non-destructively widens the application range of Laue 3DNDT to many engineering materials that exist beyond the oligocrystalline limit. This paves the way towards in-situ studies, investigating in depth deformation- and thermally-induced martensitic transformations, as well as extracting grain-resolved strain information. Additionally, varying textures in different parts of the probed volume of inhomogeneous samples related to external treatment and stimuli can be identified and analyzed in the future, complementing other traditional neutron-based diffraction methods.

4. Conclusions and outlook

Laue 3DNDT is based on forward modelling for correlating and multiple fitting of measured diffraction data originating from diffraction from a large number of individual grains. This enables not only to identify individual grains, but also their position and orientation in the sample. The feasibility of the method has been tested in several different samples. The method has been applied on engineering and functional materials and provided up to several hundred indexed grains, which enables texture evaluation with statistical relevance. A GPU-based reconstruction tool compliments the 3D Laue multi grain indexing algorithm and enables 3D grain distribution mapping and indexing of oligocrystalline samples. The proof-of-principle investigation gave good matching with ground truth measurements using EBSD.

Within an SDSC-funded program, the Applied Materials Group of LNS at PSI is currently working with the Swiss Data Science Center on developing new robust and scalable algorithms utilizing advanced data science methods, such as machine learning. Through advanced data science, the outlook of this project is to better exploit the information contained in the diffraction data and create more efficient and user friendly indexing algorithms. The FALCON instrument is foreseen to have its dedicated position in the SINQ neutron guide hall. Furthermore, the two detectors of FALCON can, like currently, be used at the POLDI instrument as add-on. First Laue3DNDT commissioning measurements at POLDI were successfully conducted in December 2021.

References

[1] M. A. Groeber, B. K. Haley, M. D. Uchic, D. M. Dimiduk, and S. Ghosh, *3D Reconstruction and Characterization of Polycrystalline Microstructures Using a FIB–SEM System*, Materials Characterization **57**, 259 (2006).

[2] S. Zaefferer, S. I. Wright, and D. Raabe, *Three-Dimensional Orientation Microscopy in a Focused Ion Beam–Scanning Electron Microscope: A New Dimension of Microstructure Characterization*, Metall and Mat Trans A **39**, 374 (2008).

[3] H. H. Liu, S. Schmidt, H. F. Poulsen, A. Godfrey, Z. Q. Liu, J. A. Sharon, and X. Huang, *Three-Dimensional Orientation Mapping in the Transmission Electron Microscope*, Science **332**, 833 (2011).

[4] G. Stechmann, S. Zaefferer, P. Konijnenberg, D. Raabe, C. Gretener, L. Kranz, J. Perrenoud, S. Buecheler, and A. N. Tiwari, *3-Dimensional Microstructural Characterization of CdTe Absorber Layers from CdTe/CdS Thin Film Solar Cells*, Solar Energy Materials and Solar Cells **151**, 66 (2016).

[5] S. Smeets, X. Zou, and W. Wan, *Serial Electron Crystallography for Structure Determination and Phase Analysis of Nanocrystalline Materials*, J Appl Crystallogr **51**, 1262 (2018).

[6] W. Zhu, G. Wu, A. Godfrey, S. Schmidt, Q. He, Z. Feng, T. Huang, L. Zhang, and X. Huang, *Five-Parameter Grain Boundary Character Distribution of Gold Nanoparticles Based on Three Dimensional Orientation Mapping in the TEM*, Scripta Materialia **214**, 114677 (2022).

[7] H. F. Poulsen, S. F. Nielsen, E. M. Lauridsen, S. Schmidt, R. M. Suter, U. Lienert, L. Margulies, T. Lorentzen, and D. Juul Jensen, *Three-Dimensional Maps of Grain Boundaries and the Stress State of Individual Grains in Polycrystals and Powders*, J Appl Cryst **34**, 751 (2001).

[8] B. C. Larson, W. Yang, G. E. Ice, J. D. Budai, and J. Z. Tischler, *Three-Dimensional X-Ray Structural Microscopy with Submicrometre Resolution*, Nature **415**, 887 (2002).

[9] D. J. Jensen, E. M. Lauridsen, L. Margulies, H. F. Poulsen, S. Schmidt, H. O. Sørensen, and G. B. M. Vaughan, *X-Ray Microscopy in Four Dimensions*, Materials Today **9**, 18 (2006).

[10] W. Ludwig, S. Schmidt, E. M. Lauridsen, and H. F. Poulsen, *X-Ray Diffraction Contrast Tomography: A Novel Technique for Three-Dimensional Grain Mapping of Polycrystals. I. Direct Beam Case*, J Appl Cryst **41**, 302 (2008).

[11] G. Johnson, A. King, M. G. Honnicke, J. Marrow, and W. Ludwig, *X-Ray Diffraction Contrast Tomography: A Novel Technique for Three-Dimensional Grain Mapping of Polycrystals. II. The Combined Case*, J Appl Cryst **41**, 310 (2008).

[12] W. Ludwig, P. Reischig, A. King, M. Herbig, E. M. Lauridsen, G. Johnson, T. J. Marrow, and J. Y. Buffière, *Three-Dimensional Grain Mapping by x-Ray Diffraction Contrast Tomography and the Use of Friedel Pairs in Diffraction Data Analysis*, Review of Scientific Instruments **80**, 033905 (2009).

[13] U. Lienert et al., *High-Energy Diffraction Microscopy at the Advanced Photon Source*, JOM **63**, 70 (2011).

[14] S. A. McDonald, P. Reischig, C. Holzner, E. M. Lauridsen, P. J. Withers, A. P. Merkle, and M. Feser, *Non-Destructive Mapping of Grain Orientations in 3D by Laboratory X-Ray Microscopy*, Sci Rep **5**, 14665 (2015).

[15] S. Peetermans and E. H. Lehmann, *Simultaneous Neutron Transmission and Diffraction Contrast Tomography as a Non-Destructive 3D Method for Bulk Single Crystal Quality Investigations*, Journal of Applied Physics **114**, 124905 (2013).

[16] R. Woracek, D. Penumadu, N. Kardjilov, A. Hilger, M. Boin, J. Banhart, and I. Manke, *3D Mapping of Crystallographic Phase Distribution Using Energy-Selective Neutron Tomography*, Advanced Materials **26**, 4069 (2014).

[17] S. Peetermans, A. King, W. Ludwig, P. Reischig, and E. H. Lehmann, *Cold Neutron Diffraction Contrast Tomography of Polycrystalline Material*, Analyst **139**, 5765 (2014).

[18] H. Sato et al., *Inverse Pole Figure Mapping of Bulk Crystalline Grains in a Polycrystalline Steel Plate by Pulsed Neutron Bragg-Dip Transmission Imaging*, J Appl Crystallogr **50**, 1601 (2017).

[19] A. Cereser et al., *Time-of-Flight Three Dimensional Neutron Diffraction in Transmission Mode for Mapping Crystal Grain Structures*, Scientific Reports **7**, 9561 (2017).

[20] M. Raventós, M. Tovar, M. Medarde, T. Shang, M. Strobl, S. Samothrakitis, E. Pomjakushina, C. Grünzweig, and S. Schmidt, *Laue Three Dimensional Neutron Diffraction*, Scientific Reports **9**, 4798 (2019).

[21] S. Samothrakitis, M. Raventós, J. Čapek, C. B. Larsen, C. Grünzweig, M. Tovar, M. Garcia-Gonzalez, J. Kopeček, S. Schmidt, and M. Strobl, *Grain Morphology Reconstruction of Crystalline Materials from Laue Three-Dimensional Neutron Diffraction Tomography*, Scientific Reports **10**, 1 (2020).

[22] G. N. Iles and S. Schorr, *The HZB Neutron Laue Diffractometer: From E11 to FALCON*, Neutron News **25**, 27 (2014).

[23] S. Samothrakitis et al., *A Multiscale Study of Hot-Extruded CoNiGa Ferromagnetic Shape-Memory Alloys*, Materials & Design **196**, 109118 (2020).

[24] N. Otsu, *A Threshold Selection Method from Gray-Level Histograms*, IEEE Transactions on Systems, Man, and Cybernetics **9**, 62 (1979).

[25] D. Bradley and G. Roth, *Adaptive Thresholding Using the Integral Image*, Journal of Graphics Tools **12**, 13 (2007).

[26] S. Schmidt, *GrainSpotter: A Fast and Robust Polycrystalline Indexing Algorithm*, J Appl Cryst **47**, 276 (2014).

[27] W. van Aarle, W. J. Palenstijn, J. De Beenhouwer, T. Altantzis, S. Bals, K. J. Batenburg, and J. Sijbers, *The ASTRA Toolbox: A Platform for Advanced Algorithm Development in Electron Tomography*, Ultramicroscopy **157**, 35 (2015).

[28] W. van Aarle, W. J. Palenstijn, J. Cant, E. Janssens, F. Bleichrodt, A. Dabravolski, J. D. Beenhouwer, K. J. Batenburg, and J. Sijbers, *Fast and Flexible X-Ray Tomography Using the ASTRA Toolbox*, Opt. Express, OE **24**, 25129 (2016).

[29] J. Trampert and J.-J. Leveque, *Simultaneous Iterative Reconstruction Technique: Physical Interpretation Based on the Generalized Least Squares Solution*, Journal of Geophysical Research: Solid Earth **95**, 12553 (1990).

[30] W. J. Palenstijn, K. J. Batenburg, and J. Sijbers, *Performance Improvements for Iterative Electron Tomography Reconstruction Using Graphics Processing Units (GPUs)*, Journal of Structural Biology **176**, 250 (2011).

[31] M. Morin et al., *Incommensurate Magnetic Structure, Fe/Cu Chemical Disorder, and Magnetic Interactions in the High-Temperature Multiferroic $YBaCuFeO_5$*, Phys. Rev. B **91**, 064408 (2015).

[32] M. Morin, E. Canévet, A. Raynaud, M. Bartkowiak, D. Sheptyakov, V. Ban, M. Kenzelmann, E. Pomjakushina, K. Conder, and M. Medarde, *Tuning Magnetic Spirals beyond Room Temperature with Chemical Disorder*, Nat Commun **7**, 1 (2016).

[33] M. C. J. Morin, Tuning Magnetic Spiral Order In Layered $RBaCuFeO_5$ Perovskites (R = Rare Earth and Y), Doctoral Thesis, ETH Zurich, 2016.

[34] S. Samothrakitis, C. B. Larsen, J. Čapek, E. Polatidis, M. Raventós, M. Tovar, S. Schmidt, and M. Strobl, *Microstructural Characterization through Grain Orientation Mapping with Laue Three-Dimensional Neutron Diffraction Tomography*, Materials Today Advances **15**, 100258 (2022).

[35] J. K. Mackenzie, *The Distribution of Rotation Axes in a Random Aggregate of Cubic Crystals*, Acta Metallurgica **12**, 223 (1964).

Announcements

SGN/SNSS Members

Presently the SGN/SNSS has 195 members. New members can register online on the SGN/SNSS website: http://sgn.web.psi.ch

SGN/SSSN Annual Member Fee

The SGN/SNSS members are kindly asked to pay their annual member fees. At the general assembly 2013 of the society, the fee has been increased from CHF 10 to **CHF 20**. It can be paid either by bank transfer or in cash during your next visit at PSI. The bank account of the society is accessible for both Swiss national and international bank transfers: Postfinance: 50-70723-6 (BIC: POFICHBE), IBAN: CH39 0900 0000 5007 0723 6.

The SGN/SSSN is an organisation with tax charitable status. All fees and donations payed to the SGN/SSSN are **tax deductible**.

PSI Facility News

Recent news and scientific highlights of the three major PSI user facilities SLS, SINQ and SμS can be found in the **quarterly electronic newsletter** available online under:
https://www.psi.ch/science/facility-newsletter

News from SINQ

With the closure of the neutron sources at HZB Berlin and LLB, Saclay, in 2019 and several other neutron sources not being online, SINQ has received a record number of proposals during the last two proposal cycles. Many proposals had to be rejected, as the over-booking factors on several instruments have doubled. With three user cycles being planned in 2023 at the ILL, the neutron beamtime situation in Europe will ease up a bit next year.

After the upgrade of the SINQ guide system, several instruments are being upgraded and are planned to join user operation during the next user cycles. The diffractometer DMC has received a new ^{3}He detector and commissioning is planned to be finished by the end of 2022. The small-angle instrument SANS-LLB is being set up at SINQ in collaboration with the Laboratoire Léon-Brillouin (Saclay, France). Hot commissioning will start in December 2022, and SANS-LLB is planned to join the user program in 2023. POLDI and NEUTRA are currently undergoing major upgrades in parallel with user operation. The new versions of POLDI and NEUTRA are currently foreseen to be operational in 2024.

Please visit the page https://www.psi.ch/sinq/call-for-proposals to obtain the latest information about beam cycles and the availability of the neutron instruments.

Registration of publications

Please remember to **register all publications either based on data taken at SINQ, SLS, SμS or having a PSI co-author** to the Digital Object Repository at PSI (DORA):
www.dora.lib4ri.ch/psi/
Please follow the link ‘Add Publication’.

Open Positions at SINQ and ILL

Open positions at SINQ or ILL are advertised on the following webpages:
https://www.psi.ch/pa/stellenangebote
https://www.ill.eu/careers/all-our-vacancies/?L=0

PhD positions at ILL

The PhD program of the Institut Laue-Langevin, ILL, is open to researchers in Switzerland. Consult the page
https://www.ill.eu/careers/all-our-vacancies/phd-recruitment
for information on the PhD program of ILL or get in contact with the managers of the program using the email address phd@ill.fr.
The Swiss agreement with the ILL includes that ILL funds and hosts one PhD student from Switzerland.

Conferences and Workshops December 2022 and beyond

An updated list with online links can be found here:
http://www.psi.ch/useroffice/conference-calendar

December 2022

FerroSchool Winter 2022
December 5-9, 2022, Calgary, Alberta, Canada

MLZ User Meeting 2022
December 8-9, 2022, Munich, Germany

6th Neutron and Muon School at J-PARC MLF and JRR-3
December 12-16, 2022, Tokai, Ibaraki, Japan

January 2023

Scientific Opportunities with very Hard XFEL Radiation
January 18-20, 2023, Hamburg, Germany

15th International Symposium on Hydrogen and Energy 2023
January 22-27, 2023, Emmetten, Switzerland

February 2023

HERCULES European School 2023
February 27 - March 31, 2023, Grenoble, France

March 2022

APS March Meeting 2023
March 6-10, 2023, Las Vegas, Nevada, USA

XXII GEM:The 22nd congress of the French Membrane Group
March 14-17, 2023, Autrans, France

Neutron and the X-ray Scattering in Materials Science symposium at the TMS 2023
March 19-23, 2023, San Diego, CA

ECNS 2023: 8th European Conference on Neutron Scattering
March 20-23, 2023, Garching, Germany

June 2023

8th European Crystallography School 2023
June 18-24, 2023, Berlin, Germany

Editorial

Editor
Swiss Neutron Science Society

Address
Sekretariat SGN/SSSN/SNSS
c/o Paul Scherrer Institut
WLGA/018
CH-5232 Villigen PSI
phone: +41 56 310 46 66
fax: +41 56 310 32 94
http://sgn.web.psi.ch

Bank Account
Postfinance: 50-70723-6 (BIC: POFICHBE)
IBAN: CH39 0900 0000 5007 0723 6

Printing
Paul Scherrer Institut
Circulation: 1600
2 numbers per year

Swiss Neutron Science Society
Sekretariat SGN/SSSN/SNSS
WLGA/018
Paul Scherrer Institut
5232 Villigen PSI, Switzerland

Join the Swiss Neutron Science Society…

to support all science using neutron radiation in Switzerland.
The Swiss Neutron Science Society is open to everybody interested in neutron scattering and research using neutron radiation in general.

The annual membership fee is CHF 20.-, but the membership is free for Bachelor-, Master-, and PhD-students.

Send an email to sgn@psi.ch to join.